

Hybrid Analogue / Digitized Radio-over-Fibre Downlink Through Orthogonal Optical mm-Wave and 10 Gb/s Baseband Transport

A. Val Martí, N. Vokić, M. Hofer, D. Milovančev, T. Zemen, B. Schrenk

AIT Austrian Institute of Technology, GG4, 1210 Vienna, Austria. aina.val-marti@ait.ac.at

Abstract We experimentally demonstrate the simultaneous radio-over-fibre transmission of an analogue 1-GHz OFDM signal on a mm-wave carrier frequency at 33 GHz and digitized 10 Gb/s data. Single-wavelength transport is supported through an intensity/phase modulation pair and a compact silicon micro-ring resonator, at <1dB penalties.

Introduction

Cloud-based signal processing in 5G infrastructures calls for efficient antenna remoting schemes. The main idea can be summarized by the fundamental principle of aggregating complex radio equipment at a centralized location while deploying the field-installed remote radio heads (RRH) as greatly simplified tail-end equipment. Optical transmission plays a critical role in off-loading radio signal processing to a cloud hostel, by connecting both, baseband radio unit and remote radio head through an – ideally – transparent optical link. Different functional split options exist towards this direction^[1]. These are advocating analogue solutions^{[2]-[5]} with high CPRI-equivalent data rates for broadband radio signals and digital schemes^[6-8] by virtue of their improved robustness to noise and non-linear distortions arising at opto-electronic interfaces such as modulators. However, there is no one-fits-all solution since radio access networks are conceived as heterogeneous networks, featuring traditional macrocell coverage paired with small cell technologies^[9]. It is therefore of practical interest to combine digitized and analogue radio-over-fibre (RoF) transmission over the same mobile fronthaul in a resource-friendly manner. Towards this direction, the polarization dimension has been exploited for the purpose of multiplexing^[10], though requiring means for polarization control. Moreover, non-orthogonal uplink transmission of baseband signals and narrow-band OFDM has been proposed together with feed-forward cancellation^[11].

In this work, we introduce orthogonal modulation in phase and intensity in order to jointly feed macro- and small-cell RRH sites in disjunct baseband (0-10 GHz) and mm-wave (33 GHz) frequencies, respectively. We evaluate this hybrid digitized/analogue RoF transmission for 10 Gb/s binary phase shift keying (BPSK), demodulated through a simple and compact silicon micro-ring resonator (MRR), and for a 1-GHz broadband 16-QAM OFDM radio transmission in the K_a-band, embedding real-

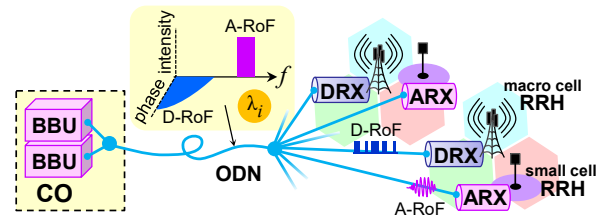


Fig. 1: Single-wavelength analogue and digitized RoF transport to macro- and small-cell RRHs.

time video transmission using software-defined radio (SDR) equipment.

Hybrid RoF over Single Wavelength

In order to support the spectrally efficient RoF integration for heterogeneous radio networks, we propose the adoption of orthogonal optical encoding for the RoF signals (Fig. 1). The main aim is to aggregate radio signals with spectrally distinct characteristics for the purpose of wavelength re-use. Such a case applies to baseband-modulated digitized and passband-modulated analogue RoF signals, which are both key to radio access networks with a mix of macro- and small cells.

Orthogonal modulation schemes based on phase and intensity modulation have been investigated for wired optical access, where they serve the purpose of remodulating a downstream wavelength with upstream data^[12]. Here, we instead exploit the orthogonality to feed two independent RoF signals over same downlink wavelength. Optical beat interference during signal detection is avoided since the frequency spectra of the phase-encoded digitized and the intensity modulated analogue RoF signals do not overlap. This condition clearly holds for the case of mm-wave analogue RoF transmission, considering its 33 GHz RF carrier frequency and the digital baseband data rate of 10 Gb/s. The intensity-modulated mm-wave analogue RoF tributary is detected with a phase-agnostic receiver. The detection of the phase-encoded, digitized RoF tributary requires an optical demodulator, for which a compact silicon MRR will be adopted. The notch function of its through-port, which is aligned to the optical

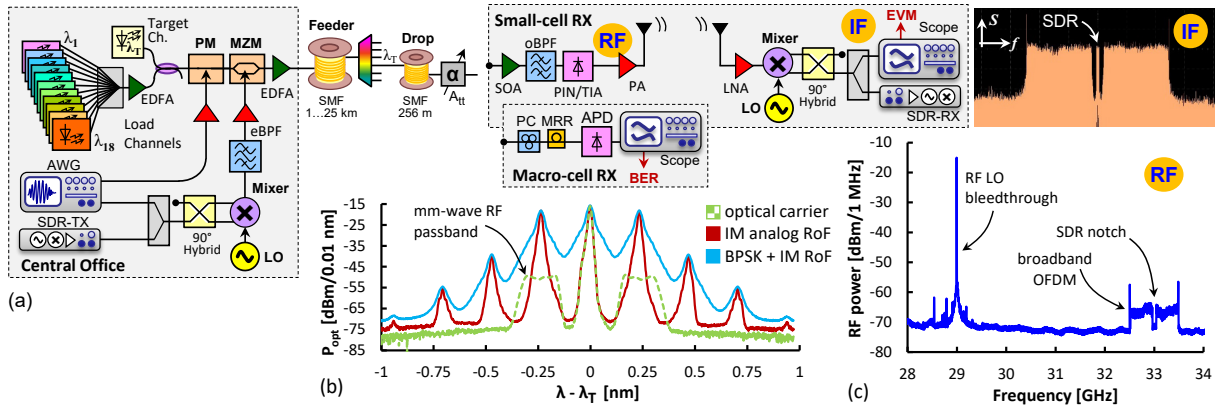


Fig. 2: (a) Experimental setup. (b) Launched optical signal spectrum at λ_T . (c) Received mm-wave RF spectrum.

carrier, leads to modulation format conversion^[13] and allows to detect the digitized RoF signal with a photodetector whose frequency response further cuts the analogue mm-wave RoF signal that is also passed through the MRR.

Experimental Setup

The experimental setup is shown in Fig. 2a. At the central office (CO), a target channel at $\lambda_T = 1550.1$ nm is combined with an 18-channel DWDM comb from 1531 to 1560 nm and sequentially modulated in phase and intensity, respectively. This yields the digitized BPSK RoF signal and the analogue mm-wave OFDM RoF signal. Generation of the signals is conducted through an arbitrary waveform generator (AWG). The 16-QAM OFDM signal with 128 sub-carriers over a bandwidth of 1 GHz at an intermediate carrier frequency of 4 GHz is up-converted by mixing it with an RF local oscillator (LO) of 29 GHz. A spectral notch is included in the broadband OFDM signal in order to embed another narrowband OFDM signal (see inset 'IF' in Fig. 2a) generated through an SDR unit and carrying a high-definition video stream with a 1920 px \times 1080 px resolution.

The DWDM signal is then launched to an optical distribution network including an arrayed waveguide grating based DWDM demultiplexer in order to form virtual point-to-point links between the CO and the RRHs.

One notable feature of the proposed architecture is that it employs two different receivers: one to demodulate the phase information at the target channel, herein referred to as the macro-cell RX, and another one, the small-cell RX, dedicated to the intensity-modulated OFDM signal.

The macro-cell RX consists of an MRR as an optical demodulator for the phase-encoded digital RoF signal, which can then be detected with an avalanche photodetector (APD) for the purpose of BER estimation. Two MRRs were fabricated on silicon-on-insulator technology

using a 220×500 nm² waveguide cross-section. Their footprints were 250×250 μm^2 (MRR₁) and 10×15 μm^2 (MRR₂). These are orders-of-magnitude smaller than delay interferometers based on micro-optics. The pass-through transfer function of the MRRs is reported in Fig. 3a. The free spectral ranges (FSR) of the MRRs were 120.5 GHz and 2.42 THz respectively, which renders the larger MRR₁ to be in better alignment with the DWDM grid. The Q-factors were 27.7k and 18.8k. A peak extinction of more than 23.4 dB has been achieved. Fibre-to-waveguide coupling was accomplished through single-polarization grating couplers, yielding a fibre-to-fibre loss of -12.8 to -11.7 dB.

The small-cell RX employs a 40G PIN/TIA receiver that is optically pre-amplified with a semiconductor optical amplifier (SOA), whose amplified spontaneous emission tails have been suppressed by a CWDM optical bandpass filter (BPF). The detected 33 GHz OFDM signal is amplified and transmitted over an mm-wave freespace link, using directional antennas with a gain of 20 dB spaced by 2 meters. The radio signal is then down-converted, digitized and evaluated. Real-time video transmission and off-line EVM estimation have been conducted for the purpose of performance evaluation.

Analogue / Digitized RoF Performance

The optical spectrum of the transmitted signal, relative to the target wavelength, is shown in Fig. 2b for the cases of intensity and orthogonal modulation. The characteristic double-sideband passband spectrum of the mm-wave radio broadens for the additional phase modulation in the baseband. The received electrical spectrum of the analogue radio-over-fibre signal after photodetection (RF) is presented in Fig. 2c. Besides the 1-GHz OFDM signal with the two pilot tones at its spectral boundaries there is a considerable bleed-through from the RF LO, which is subject to further improvement.

Analogue RoF: The performance for the

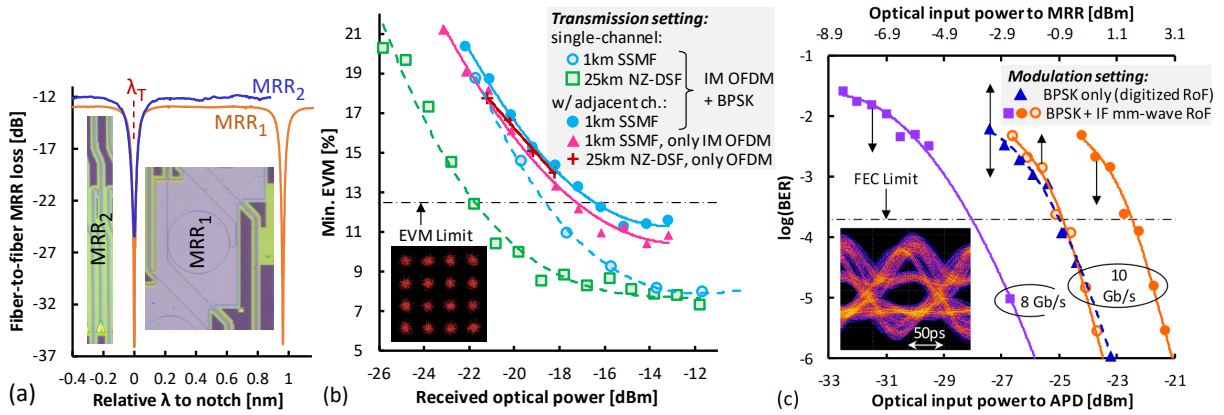


Fig. 3: (a) MRR transfer functions. (b) EVM for analogue mm-wave OFDM RoF reception. (c) BER for digitized RoF transmission.

analogue RoF transmission is presented in Fig. 3b in terms of error vector magnitude (EVM) for the broadband 1-GHz OFDM signal as a function of the input power to the small-cell SOA+PIN receiver. Due to the dispersion-limited transmission of the double-sideband mm-wave signal, a short feeder length of 1 km has been chosen. For single-channel transmission and simultaneous digitized and analogue RoF transmission, an EVM of 8% can be accomplished and the EVM limit of 12.5% for 16-QAM transmission is reached at a received optical power of -18.7 dBm (○). In presence of 18 adjacent DWDM channels, the minimum EVM is increased to 11.2% (●). This is attributed to the loading of the booster EDFA, which leads to a degraded OSNR. The reception penalty due to the simultaneous digitized and analogue RoF transmission over the same wavelength is 0.8 dB at the EVM limit (▲,●). Real-time video transmission over the embedded narrowband mm-wave link was accomplished without visual artifacts (Fig. 4). We further achieved analogue RoF transmission below the EVM limit over 25 km of NZ-DSF feeder under single-channel conditions (□). However, the loading of the booster amplifier with adjacent channels (+) reduces the launched power per channel, which renders the power budget as too restricted to accomplish reception below the EVM limit for the given optical mm-wave receiver. The optical and electrical back-to-back EVM were 6.4% and 4.2%, respectively.

Digitized RoF: The transmission performance of the digitized RoF transmission over 4.3 km after phase demodulation with the MRR at the macro-cell RX is presented in Fig. 3c in terms of BER. For the large MRR₁ with a periodicity of its notch function close to that required for DWDM, 10 Gb/s transmission was subject to an error floor due to its spectral characteristics. 8 Gb/s was accomplished at a reception sensitivity of -28.1 dBm at the FEC threshold of 2.10^{-4} (■)



Fig. 4: Real-time video transport embedded in mm-wave RoF.

when referring to the APD input. For the smaller MRR₂ with wider FSR, 10 Gb/s was achieved at a sensitivity of -24.8 dBm (▲). When activating the analogue RoF feed, the sensitivity degrades by 2.4 dB (●). However, this is because the mm-wave signal now falls at the pass region of the MRR, leading to higher input power to the APD. The input power has been therefore also referenced to the input of the MRR, where the penalty due to simultaneous digitized and analogue RoF transmission is now 0.3 dB for the received digitized RoF signal (▲,○). In order to ensure this small penalty, the intensity modulator at the CO has to be strictly operated in its quadrature point to avoid non-linear beat terms of the analogue mm-wave RoF signal to interfere with the baseband digitized RoF signal.

Conclusions

We have demonstrated the use of orthogonal modulation to realize a hybrid analogue/digitized RoF downlink. Crosstalk for 1-GHz OFDM transmission at a mm-wave frequency of 33 GHz due to simultaneous baseband 10 Gb/s BPSK transmission, and vice versa, has been proven to be less than 1 dB. The integration of uplink data and dispersion tolerant analogue mm-wave transport is left for further investigation.

Acknowledgements

This work was supported in part by the ERC under the EU Horizon-2020 programme (grant n° 804769) and by the Austrian FFG agency (grant n° 883894).

References

- [1] I. A. Alimi, A. L. Teixeira and P. P. Monteiro, "Toward an Efficient C-RAN Optical Fronthaul for the Future Networks: A Tutorial on Technologies, Requirements, Challenges, and Solutions", *IEEE Communications Surveys & Tutorials*, vol. 20, no. 1, pp. 708-769, Firstquarter 2018.
- [2] H. N. Parajuli, H. Shams, L. Guerrero Gonzalez, E. Udvary, C. Renaud, and J. Mitchell, "Experimental demonstration of multi-Gbps multi sub-bands FBMC transmission in mm-wave radio over a fiber system", *Opt. Express* 26, 7306-7312 (2018).
- [3] M. Sung *et al.*, "RoF-Based Radio Access Network for 5G Mobile Communication Systems in 28 GHz Millimeter-Wave", in *Journal of Lightwave Technology*, vol. 38, no. 2, pp. 409-420, 15 Jan.15, 2020.
- [4] J. Beas, G. Castanon, I. Aldaya, A. Aragon-Zavala and G. Campuzano, "Millimeter-Wave Frequency Radio over Fiber Systems: A Survey", in *IEEE Communications Surveys & Tutorials*, vol. 15, no. 4, pp. 1593-1619, Fourth Quarter 2013.
- [5] N. Argyris *et al.*, "A 5G mmWave Fiber-Wireless IFOF Analog Mobile Fronthaul Link With up to 24-Gb/s Multiband Wireless Capacity", in *Journal of Lightwave Technology*, vol. 37, no. 12, pp. 2883-2891, 15 June15, 2019.
- [6] H. Li *et al.*, "Real-Time 100-GS/s Sigma-Delta All-Digital Radio-Over-Fiber Transmitter for 22.75–27.5 GHz Band", *2019 Optical Fiber Communications Conference and Exhibition (OFC)*, 2019, pp. 1-3.
- [7] J. Wang *et al.*, "Digital mobile fronthaul based on delta-sigma modulation for 32 LTE carrier aggregation and FBMC signals", in *IEEE/OSA Journal of Optical Communications and Networking*, vol. 9, no. 2, pp. A233-A244, Feb. 2017.
- [8] L. Zhang *et al.*, "Toward Terabit Digital Radio over Fiber Systems: Architecture and Key Technologies", in *IEEE Communications Magazine*, vol. 57, no. 4, pp. 131-137, April 2019.
- [9] T. E. Bogale and L. B. Le, "Massive MIMO and mmWave for 5G Wireless HetNet: Potential Benefits and Challenges", in *IEEE Vehicular Technology Magazine*, vol. 11, no. 1, pp. 64-75, March 2016.
- [10] S. Shen *et al.*, "Polarization-tracking-free PDM supporting hybrid digital-analog transport for fixed-mobile system," *IEEE Photon. Technol. Lett.*, vol. 31, no. 1, pp. 54–57, Jan. 2019.
- [11] S. Yao *et al.*, "Non-Orthogonal Uplink Services Through Co-Transport of D-RoF/A-RoF in Mobile Fronthaul," in *Journal of Lightwave Technology*, vol. 38, no. 14, pp. 3637-3643, 15 July15, 2020.
- [12] Y. Zhang, N. Deng, C.K. Chan, and L.K. Chen, "A Multicast WDM-PON Architecture Using DPSK/NRZ Orthogonal Modulation", *IEEE Photonics Technol. Lett.*, vol. 20, pp. 1479-1481, Sept. 2008.
- [13] L. Zhang, J. Y. Yang, M. Song, Y. Li, B. Zhang, R. G. Beausoleil, and A. E. Willner, "Microring-based modulation and demodulation of DPSK signal", *Opt. Express* 15(18), 11564–11569 (2007).